Rapid Recovery of Male Cats with Postrenal Acute Kidney Injury by Treating with Allogeneic Adipose Mesenchymal Stem Cell-derived Exosomes

Weihui Li
Northwest A&F University: Northwest Agriculture and Forestry University
Wei Wang
Northwest A&F University: Northwest Agriculture and Forestry University
Xin He
Northwest A&F University: Northwest Agriculture and Forestry University
Zheng Liao
Northwest A&F University: Northwest Agriculture and Forestry University
Aili Aierken
Northwest A&F University: Northwest Agriculture and Forestry University
Jinlian Hua
Northwest A&F University: Northwest Agriculture and Forestry University
Yan Wang
Northwest A&F University: Northwest Agriculture and Forestry University
Dezhang Lu
Northwest A&F University: Northwest Agriculture and Forestry University
Shiqiang Zhang (shiqiangzhang@nwsuaf.edu.cn)
Northwest A&F University: Northwest Agriculture and Forestry University https://orcid.org/0000-0002-0414-4365

Research Article

Keywords: Acute kidney injury, Mesenchymal stem cells, Exosomes, Cat

Posted Date: April 8th, 2022

DOI: https://doi.org/10.21203/rs.3.rs-1453150/v1

Abstract

Background: Acute kidney injury (AKI) is a complex disease and can be generally divided into prerenal, intrarenal, and postrenal AKI (PR-AKI). Previous studies have shown that mesenchymal stem cells (MSCs)-derived exosomes have protective function on prerenal and intrarenal AKI treatment, but whether they have therapeutic efficacy on PR-AKI remains unclear. In this study, we investigated the therapeutic efficacy of allogeneic adipose mesenchymal stem cells-derived exosomes (ADMSCEs) on a cat model of PR-AKI.

Methods: The cat models of PR-AKI were established by using artificial urinary occlusion and then treated with ADMSCEs. Histopathological section analysis, blood routine analysis, plasma biochemical test, imaging analysis, and plasma ultra-high performance liquid chromatography-MS/MS (UHPLC-MS/MS) were performed to evaluate the therapeutic efficacy of ADMSCEs.

Results: Physiological and biochemical test showed that the ADMSCEs could recover creatinine, urea nitrogen and plasma phosphorus to homeostasis efficiently. Blood routine analysis showed that leukocytes in PR-AKI cats with ADMSCEs treatment returned to normal physio-logical range more quickly than that of control. UHPLC-MS/MS analysis revealed that the plasma metabolome profile of PR-AKI cats treated with ADMSCEs was highly similar to that of normal cats. Furthermore, UHPLC-MS/MS analysis also revealed six metabolites (carnitine, melibiose, D−glucosamine, cytidine, dihydroorotic acid, stachyose) in plasma were highly correlated with the dynamic process of PR-AKI on cats and were potential novel targets for ADMSCEs therapy.

Conclusions: Our findings demonstrate the efficacy of ADMSCEs in the treatment of PR-AKI on cats, and provide valuable reference for translational medicine research on PR-AKI treatment in elderly patients with MSCs-derived exosomes in the future.

1. Introduction

Acute kidney injury (AKI), also called acute renal failure, is a serious, rapid and complex disorder of kidney damage in human. The incidence rate of AKI is between 1/10000 and 6/10000 per year in the community setting [1]. According to the etiology, AKI can be generally divided into prerenal, intrarenal, and postrenal (PR-AKI). The main causes of prerenal AKI include decreased blood volume (such as massive hemorrhage and severe dehydration), heart failure (insufficient renal perfusion caused by decreased cardiac output), shock or the use of high-dose vasodilators. Intrarenal AKI occurs when direct damage to the kidneys, and is common in glomerular disease, tubulointerstitial disease, and nephrovascular disease. By contrast, PR-AKI occurs when an obstruction in the urinary tract causes the waste to build up in the kidneys. PR-AKI accounts for about 10% of AKI, especially in elderly patients, the proportion of PR-AKI is up to 22%[2].

Male cats are a good model to study PR-AKI, since male cats have a long and narrow urethra, which is easy to induce urinary obstruction due to stress. The clinical symptoms of PR-AKI in cats are highly

similar to those in humans. In clinical veterinary medicine, the proportion of PR-AKI in male cats is as high as 65%. The mortality rate for PR-AKI in cats is also high, approaching 47%. Of the survived individuals, nearly 60% male cats developed chronic renal failure[3].

In mice and rats, previous studies have shown that mesenchymal stem cells-derived exosomes (MSCEs) can effectively treat prerenal and intrarenal AKI [4, 5]. So far, there are no reports of MSCEs in the treatment of PR-AKI. It is not clear whether MSCEs are effective in the treatment of PR-AKI. In this study, we investigated the efficacy of allogenic adipose mesenchymal stem cells-derived exosomes (ADMSCEs) on the cat model of PR-AKI. Through physiological and biochemical analysis, blood routine analysis and plasma metabolome analysis, we proved the effectiveness of ADMSCEs in the treatment of PR-AKI. Furthermore, we revealed the potential metabolite targets of ADMSCEs in the treatment of PR-AKI. In short, our study provides valuable reference and clue for translational medicine research on the treatment of human PR-AKI with mesenchymal stem cells-derived exosomes in the future.

2. Materials And Methods

2.1 Isolation and culture of ADMSCs

The healthy experimental female cats (three months old, weighing 2kg) were used for isolation of adipose mesenchymal stem cells. After anesthesia, the adipose tissue on both sides of cat's the groin was taken aseptically and cut into 1mm3 pieces for collagenase digestion. Type 1 collagenase (Gibco) (0.1%) was added to the tissue pieces and incubated at 37 ℃ for one hour. Then the supernatant was discarded by centrifuging at 250 g for 5 min. The cell pellets were resuspended with 5 ml medium and screened with 100 mesh filter. Finally, the cell pellets were collected by centrifugation (250 g, 5 min) again and cultured with ADMSCs medium (88% MEM basal medium (Gibco), 1% penicillin and streptomycin (Gibco), 1% glutamine (Gibco) and 10% fetal bovine serum (Biological Industries)). After 24 hours, non-adherent cells were removed and replaced with the fresh ADMSCs medium. When the ADMSCs growth confluence reached 80%, the cells were trypsinized and collected for liquid nitrogen cryopreservation. In this study, ADMSCs within four passages after thawing were used for subsequent treatment trials.

2.2 Differentiation of ADMSCs and characterization

Osteogenic differentiation: The ADMSCs at passage 4 were cultured in a 12-well plate with ADMSCs medium. When the cells growth reached 60% confluence, the ADMSCs were replaced with osteogenic differentiation medium (MEM medium containing 10% FBS, 100 nM dexamethasone (Selleck), 30 μg/ml ascorbic acid (sigma) and 10 mM sodium ß-glycerophosphate (solarbio)) and induced to differentiation for 14 days. After that, the cells were fixed with 4% paraformaldehyde, washed with PBS, and incubated with alizarin red staining solution for 30 minutes. Finally, cells are used for photography after removing alizarin red staining solution and washing with PBS for three times.

Adipogenic differentiation: The ADMSCs were cultured similarly as above, then ADMSCs were replaced with adipogenic differentiation medium (MEM medium containing 10% FBS, 5% Insulin-Transferrin-

Selenium-Ethanolamine (ITS-X) (Selleck), 1μM dexamethasone (Selleck) and 0.5mM 3-Isobutyl-1-methylxanthine (IBMX) (Selleck)). After 14 days' differentiation, the cells were fixed with 4% paraformaldehyde, washed with PBS, and incubated with oil red O staining solution (solarbio) for 60 minutes. Finally, cells are used for photography after removing staining solution and washing with PBS for three times.

2.3 Isolation and identification of ADMSCs-derived exosomes

The ADMSCs were cultured in a 100 mm petri dish up to the fourth passage with ADMSCs medium. When the cells grew to a density of 80%-90% confluence, they were cultured in UltraGRO™-PURE (Helios)for 24h and cell supernatant was collected for exosome extraction with the TransExo® Cell Media Exosome Kit (TransGen biotech). The extracted exosomes were observed by electron microscope size analysis. The exosome pellets were lysed, and immunoblotted for TSG101 (Wanleibio)and CD63 (Wanleibio).

2.4 Histopathological section analysis

Kidneys were surgically dissected from the experimental cats. Samples were fixed in PBS containing 4% formaldehyde, and embedded in paraffin. Sections preparation was performed in Xi 'an Animal Hospital of Northwest Agriculture and Forestry University, and were stained with hematoxylin and eosin.

2.5 Animal model of postrenal acute renal injury and treatments

All experimental male cats (weighing 2.5kg-3.5kg) underwent physical examination, renal function examination, vaccination, deworming, and were raised in a quiet environment for one week to reduce stress response before surgery. To establish an artificial model of PR-AKI, venous access was established first, and then propofol anesthesia was performed. After anesthesia, the cat's penis was shaved and disinfected with iodophor. The catheter with a diameter of 1.3mm was inserted completely into the urethra. After that, the catheter was closed with heparin cap. Furthermore, the catheter was sutured to the foreskin to prevent it from falling off. The plasma of experimental cats was tested by Fuji-biochemical apparatus, and the blood routine was determined by Mindray four-classification blood routine apparatus. After 24 hours of artificial urinary occlusion, the cats with plasma creatinine value exceeded 770μM were identified as a successful model of postrenal acute renal injury for subsequent treatment trials.

For treatment trials, the cats were firstly relieved from urinary closure, but retained the urinary catheter. Six experimental cats were randomly divided into two groups: control treatment group and exosomes treatment group. The control treatment group was infused with anti-inflammatory drugs (ceftiofuroxime sodium, 5mg/kg), energy fluids (5% glucose) and 0.9% sodium chloride. The total amount of infusion liquid was calculated as 50 mL/kg weight + daily urine volume (mL), and the infusion speed was 10 mL /kg/h. The exosomes treatment group was infused with 10 million ADMSCs-derived exosomes beyond the components of general treatment for each cat. The preparation of exosomes was described as above.

During the treatment period, venous blood was collected every day for biochemical test and metabolomics analysis.

2.6 UHPLC-MS/MS analysis

Plasma samples of cats were thawed at 4℃, and 100 μL was taken from each sample, and mixed with 100 μL of pre-cooled ultrapure water and 800μL of pre-cooled methanol/acetonitrile (1:1, V/V). Ultrasound was performed in ice bath for 60 min, then the mixture was then incubated at -20℃ for 2h, and centrifuged at 16000g at 4℃ for 30min. The supernatants were evaporated in a high-speed vacuum concentration centrifuge. The pellets were re-dissolved with 100μL acetonitrile-water solution (1:1, v/v), centrifuged at 16000g for 20min at 4℃, and the supernatant was taken for UHPLC-MS/MS analysis.

During the whole UHPLC-MS/MS analysis, the samples were placed in an automatic sampler at 4℃, metabolomics profiling was analyzed using a UPLC-ESI-Q-Orbitrap-MS system (UHPLC, Shimadzu Nexera X2 LC-30AD, Shimadzu, Japan) coupled with Q-Exactive Plus (Thermo Scientific, San Jose, USA). The injection volume was 3 μL, the column temperature was 25℃, and the flow rate was 0.3 mL/min. Chromatographic mobile phase A: water plus 25 mM ammonium acetate, B: 100% acetonitrile. The chromatographic gradient elution procedure was as follows: the gradient was 95% B for 1 min and was linearly reduced to 65% in 7 min, and then reduced to 35% in 2 min and maintained for 1 min, and then increased to 95% in 0.5 min, with 2 min re-equilibration period employed.

2.7 Mass spectrum acquisition

The positive (+) and negative (-) modes of each sample were detected by electrospray ionization (ESI). The samples were separated by UPLC and analyzed by MASS spectrometry using QE Plus Mass Spectrometer (Thermo Scientific). The HESI source conditions were set as follows: Spray Voltage□3.8kv □+□and 3.2kv□-□□Capillary Temperature□320□±□□Sheath Gas□30□±□□Aux Gas□5□±□□Probe Heater Temp□350□±□□S-Lens RF Level□50.

Mass spectrometry collection time was 12min. Parent ion scanning range: 80-1200 m/z, primary mass spectrometry resolution: 70000 @m/z 200, AGC target: 3e6, primary maximum injection time: 100 ms. The secondary mass spectrum analysis was collected according to the following methods: isolation window was set to 2 m/z, maximum injection time: 50 ms, and the normalized collision energy (stepped) was set as 27, 29 and 32 for fragmentation.

Quality control (QC) samples were prepared by pooling aliquots of all samples that were representative of the samples under analysis, and used for data normalization.

2.8 Metabolomics data preprocessing, filtering and analysis

MSDIAL software was used for peak alignment, retention time correction and peak area extraction for the raw data. The metabolites were identified by accuracy mass (mass tolerance < 0.01Da) and MS/MS data (mass tolerance < 0.02Da) which were matched with HMDB, MassBank, and self-built metabolite standard library generated by Shanghai Bioprofile Biological Technology Co., LTD.

In the extracted-ion features, only the variables having more than 50% of the nonzero measurement values in at least one group were kept. The positive and negative ion peaks were integrated and R software was used for pattern recognition. The data were pre-processed by United Universe scaling (UV). Further data analysis, including principal component analysis (PCA), differential metabolite analysis, and KEGG pathway screening, were performed by Metaboanalysis 5.0. And the rest of the data was analyzed by Graph Pad Prism 6.0.

3. Results

3.1. Urethral obstruction in male cats mimics the clinical symptoms of PR-AKI

To make a cat PR-AKI model, we inserted the catheter into urethra of a male cat and closed the heparin cap for artificial urinary closure (AUC) (Fig. 1A). Creatinine levels in blood was monitored for 48 hours. AKI was classified into five grades based on creatinine level proposed by International Renal Interest Society. About nine hours after AUC, blood creatinine reached the level of grade III AKI. About 30 h after AUC, blood creatinine reached the level of grade IV AKI. In this study, the blood creatinine level of 770 μM was set as the lower limit standard of PR-AKI on cat disease models, which took about 35h after AUC (Fig. 1B). B ultrasonic examination showed that the kidney and ureter of cat with PR-AKI both enlarged when compared to normal state (Fig. 1C). Furthermore, the HE staining of renal slice showed obvious lesions (Fig. 1D-E).

3.2. Therapeutic efficacy of allogeneic adipose mesenchymal stem cells-derived exosomes on PR-AKI

To investigate the therapeutic efficacy of allogeneic adipose mesenchymal stem cells-derived exosomes (ADMSCEs) on PR-AKI, we first carried out quality control and identification of ADMSCEs. The isolated ADMSCs had a typical mesenchymal-like morphology and could differentiate into adipocytes and osteoblasts (Fig. 2A). ADMSCs with the above differentiation potential and within the fourth passage in vitro were used for subsequent exosome isolation. Transmission electron micrographs of ADMSCEs showed that the diameter of exosomes was in the range of 40–100 nm (Fig. 2B). Western blotting showed that ADMSCEs expressed the marker proteins TSG101a and CD63 (Fig. 2C). The whole process of treatments is shown in Fig. 2D. During the whole process of ADMSCEs treatment, we monitored the parameters of blood routine and blood biochemistry and investigated the improvement of PR-AKI. The PR-AKI cats with ADMSCEs treatment returned to normal physiological levels more quickly than that with control treatment within 72 h in terms of leukocyte count (Fig. 2E). Of note, ADMSCEs treatments restored the AKI cats to normal physiological levels more quickly than control treatments in terms of creatinine, urea nitrogen, plasma phosphorus (Fig. 2F-H). There was no difference in body temperature between the two treatment groups (Fig. 2I). In terms of plasma calcium level, we did not find significant differences between ADMSCEs and control treatment (Fig. S1A).In addition, clinical symptoms of ADMSCEs-treated

cats were also significantly improved (Table S2). In short, ADMSCEs therapy can significantly promote the recovery of PR-AKI on cats.

3.3. Plasma metabolomic analysis of PR-AKI cats treated by ADMSCEs

To comprehensively evaluate the efficacy of exosomes in the treatment of PR-AKI, we performed a paired plasma metabolomic analysis of cats at normal physiology, PR-AKI, and ADMSCEs treatment. We identified 10145 positive ion features and 6607 negative ion features by ultra-high-performance liquid chromatography-MS/MS (UHPLC-MS/MS). Due to the limitation of ion library annotation, we got 460 annotated chemicals for 10145 positive ion features and mapped these 460 chemicals on 192 KEGG pathways. In parallel, we got 348 annotated chemicals for 6607 negative ion features and mapped these 348 chemicals on 162 KEGG pathways (Table S1).

Principal component analysis of both positive ion features and negative ion features showed that the ADMSCEs treatment group and the normal physiological group were clustered together, while the AKI group was separated alone (Fig. 3A-B). In terms of annotated chemicals from positive ion features, AKI group caused increase of 111 chemicals and decrease of 35 chemicals compared with normal physiological group ($P < 0.05$, VIP > 1, Fold Change > 1.5, the same criteria were applied thereafter) (Fig. 3C). By contrast, ADMSCEs treatment group caused only increase of 20 chemicals and decrease of 17 chemicals compared with normal physiological group (Fig. 3D). In parallel, AKI group caused increase of 35 chemicals and decrease of 51chemicals compared with normal physiological group in terms of annotated chemicals from negative ion features (Fig. 3E). In sharp contrast, ADMSCEs treatment group caused only increase of 13 chemicals and decrease of 11 chemicals compared with normal physiological group (Fig. 3F). In short, these results suggest that ADMSCEs therapy effectively restored the plasma metabolome of cats with PR-AKI to a level highly similar to normal physiological homeostasis.

3.4. Potential chemical targets of ADMSCEs therapy for PR-AKI

Then we explored the potential chemical targets of ADMSCEs therapy for PR-AKI. KEGG analysis was performed for positive-ion-features-derived chemicals significantly upregulated in PR-AKI group versus normal. We found that six metabolic pathways were significantly enriched, including beta − alanine metabolism, galactose metabolism, fatty acid degradation, amino sugar and nucleotide sugar metabolism, histidine metabolism, and lysine degradation. A total of nine chemicals were found to mapped on these six pathways (Fig. 4A). In parallel, KEGG analysis was performed for chemicals significantly downregulated in ADMSCEs treatment group versus PR-AKI group. We found that five metabolic pathways were significantly enriched, including cysteine and methionine metabolism, galactose metabolism, vitamin B6 metabolism, amino sugar and nucleotide sugar metabolism, and lysine degradation. A total of seven chemicals were found to map on these five pathways (Fig. 4B). We hypothesized that chemicals satisfying the following criteria at the same time were the potential targets of ADMSCEs therapy for PR-AKI: (1) When compared with the normal control group, the chemicals

enriched in the pathways significantly upregulated in PR-AKI group; (2) when compared with PR-AKI, chemicals enriched in pathways significantly downregulated in ADMSCEs treatment group. A total of three chemicals (carnitine, melibiose, D − glucosamine) met the above three criteria.

Similarly, KEGG analysis was performed for negative-ion-features-derived chemicals significantly upregulated in PR-AKI group versus normal. We found that two metabolic pathways were significantly enriched, including pyrimidine metabolism, and galactose metabolism. A total of three chemicals were found to map on these two pathways (Fig. 4C). Meanwhile, KEGG analysis was performed for chemicals significantly downregulated in ADMSCEs treatment group versus PR-AKI group. We found that three metabolic pathways were significantly enriched, including galactose metabolism, pyrimidine metabolism, and tryptophan metabolism. A total of four chemicals were found to map on these three pathways (Fig. 4D). We used the same screening criteria as described above and revealed three negative-ion-features-derived chemicals (cytidine, dihydroorotic acid, stachyose) as the potential targets of ADMSCEs therapy for PR-AKI. Furthermore, the heatmap clearly shows expression patterns of these six candidate chemicals in normal physiological homeostasis, PR-AKI and ADMSCEs treatment (Fig. 4E).

Conversely, we also assumed that chemicals satisfying the following conditions could be potential targets for exosomes therapy for PR-AKI: (1) when compared with the normal control group, the chemicals enriched in the pathways significantly downregulated in AKI group; (2) when compared with AKI, chemicals enriched in pathways significantly upregulated in exosomes treatment group. However, we did not find any chemicals that met these conditions (Fig. S1B-E).

In summary, six chemicals were identified as potential targets for ADMSCEs in the treatment of PR-AKI, which provides clues to develop new therapeutic drugs.

3.5. Regression analysis of six candidate chemicals to PR-AKI clinical indicators

To evaluate the indicative role of six candidate chemicals in the treatment of PR-AKI by ADMSCEs, we performed Pearson correlation coefficient analysis for six candidate chemicals (carnitine, melibiose, D − glucosamine, cytidine, dihydroorotic acid, stachyose) and clinical indicators of PR-AKI (creatinine, urea nitrogen, plasma phosphorus). The heatmap showed that the six candidate chemicals were strongly correlated with creatinine, urea nitrogen, and plasma phosphorus (Fig. 5A).

Furthermore, we carried out linear regression analysis between six candidate chemicals and creatinine, respectively. There was a high linear regression between the three chemicals (carnitine, D − glucosamine, dihydroorotic acid) and creatinine ($R2 > 0.9$) (Fig. 5B). Interestingly, these three chemicals also showed a high linear regression with urea nitrogen ($R2 > 0.9$) (Fig. 5C). In contrast, only D − glucosamine showed a high linear regression with plasma phosphorus ($R2 > 0.9$) (Fig. 5D). The results above reveal that the six chemicals can be used as complementary indicators to determine the dynamic process of PR-AKI occurrence and cure in the future.

4. Discussion

In this study, the cat model of PR-AKI was used to prove for the first time that ADMSCEs can effectively promote the repair of PR-AKI. Furthermore, the plasma metabolome study of cats treated with exosomes revealed that six metabolic compounds (carnitine, melibiose, D – glucosamine, cytidine, dihydroorotic acid, stachyose) were potential targets for ADMSCEs in the treatment of PR-AKI (Fig. 6).

Carnitine is a quaternary ammonium compound. The main physiological function of carnitine is to transfer long-chain fatty acids to mitochondria for oxidation, thereby producing energy. In addition, carnitine is involved in removing metabolites from cells[6]. At organ level, kidney is the main regulator of plasma carnitine homeostasis. It has been reported that carnitine has a protective effect on AKI caused by ischemia-reperfusion[7]. In this study, the level of carnitine in PR-AKI cats increased sharply, which may be caused by the disturbance of carnitine homeostasis. The rise of carnitine in cats with PR-AKI may also be a self-protective mechanism. In addition, the highly consistent linear regression between carnitine and creatinine / urea nitrogen suggests that carnitine can be used as a new marker for PR-AKI in the future.

D -Glucosamine is a monosaccharide that contains an amine group in place of one of the hydroxyl groups. Glucosamine is an effective drug in the treatment of osteoarthritis[1]. Glucosamine can cause apoptosis in kidney tubular and mesangial cells as well as overexpression of transforming growth factor β1 (TGF-β1) and connective-tissue growth factor (CTGF), which are potent inducers of mesangial and interstitial tubulointerstitial fibrosis[8]. Therefore, we speculate that glucosamine may be one of the main agents causing PR-AKI in this study.

Dihydroorotic acid and cytidine are two substances in pyrimidine metabolism, in which dihydroorotic acid is mainly involved in nucleotide anabolism, while cytidine is produced by nucleotide catabolism. Orotic acid is a downstream metabolite of dihydroorotic acid. When the urea cycle is interrupted, orotic acid synthesis is supposed to increase. The synthesis of orotic acid is initiated by the formation of carbamyl phosphate in the cytoplasm, where the ammonia comes from glutamine. In mammals, carbamyl phosphate is formed in the first step of mitochondrial urea synthesis in the liver. In PR-AKI, the body's ability to detoxify ammonia is insufficient, resulting in the accumulation of urea nitrogen. Carbamyl phosphate leaves the mitochondrial urea synthesis pathway and enters the pyrimidine pathway to stimulate the biosynthesis of orotic acid, which may lead to the rise of dihydroorotic acid[9]. The correlation analysis between dihydroorotic acid and urea nitrogen also supports this speculation. In PR-AKI, there is a lot of cell damage, so that a lot of nucleotides need to be broken down, which may be responsible for the rise of cytidine.

Melibiose and stachyose are the products of galactose metabolism, and stachyose is the precursor of melibiose. Meliciose has been shown to effectively inhibit oxidative stress and the upregulation of inflammatory factors in mice[10, 11], while stachyose has also been shown to inhibit inflammation[12, 13]. In the case of PR-AKI, the upregulation of melibiose and stachyose may be a spontaneous protective mechanism, and the mechanism of how exosomes regulate this process needs to be further studied.

5. Conclusions

In conclusion, we demonstrated the efficacy of ADMSCEs in the treatment of PR-AKI, and revealed potential targets of ADMSCEs in the treatment of PR-AKI. The findings of this study will provide new clues for improving the clinical treatment of patients with PR-AKI.

Abbreviations

Abbreviations	Full name
AKI	Acute kidney injury
PR-AKI	Postrenal acute kidney injury
ADMSCEs	Adipose mesenchymal stem cells-derived exosomes
ADMSCs	Adipose mesenchymal stem cells
MSCEs	Mesenchymal stem cells-derived exosomes
AUC	Artificial urinary closure
UHPLC-MS/MS	Ultra-high-performance liquid chromatography-MS/MS
TGF-β1	Transforming growth factor β1
CTGF	Connective-tissue growth factor
ESI	Electrospray ionization
QC	Quality control
UV	United Universe scaling
PCA	Principal component analysis

Declarations

Acknowledgements

The author would like to thank Dr. Wu Qiaoxing for the pathological analysis of this study and all the staff in Xi 'an Animal Hospital of Northwest A&F University for their help in the animal experiment part of this study.

Funding

This research was funded by Xi'an Animal Hospital of Northwest A&F University (K4040121234).

Availability of data and materials

Not applicable.

Ethics approval and consent to participate

The authors are accountable for all aspects of the work in ensuring that questions related to the accuracy or integrity of any part of the work are appropriately investigated and resolved. All animal tests were approved by the Experimental Animal Committee of the Northwest A&F University and were conducted in accordance with the Guidelines for Experimental Animals of the Ministry of Science and Technology (Beijing, China).

Competing interests

The authors declare that they have no competing interests.

Consent for publication

Not applicable.

Authors' contributions

Conceptualization W.L., Y.W., D.L., S.Z.; Methodology W.L., W.W., X.H., Z.L., A.A.; Investigation W.L., W.W.; Original draft preparation W.L., W.W., Y.W., D.L., S.Z;Writing review and editing W.L., J.H., X.Z., Y.W., D.L., S.Z; Supervision Y.W., D.L., S.Z.. All authors have read and agreed to the published version of the manuscript.

Authors' information

Weihui Li, College of Veterinary Medicine, Northwest A&F University, Yangling (712100), China.

Wei Wang, College of Veterinary Medicine, Northwest A&F University, Yangling (712100), China.

Xin He, College of Veterinary Medicine, Northwest A&F University, Yangling (712100), China.

Zheng Liao, College of Veterinary Medicine, Northwest A&F University, Yangling (712100), China.

Aili Aierken, College of Veterinary Medicine, Northwest A&F University, Yangling (712100), China.

Jinlian Hua, College of Veterinary Medicine, Northwest A&F University, Yangling (712100), China.

Shiqiang Zhang, College of Veterinary Medicine, Northwest A&F University, Yangling (712100), China.

Dezhang Lu, Xi'an Animal Hospital, Northwest A&F University

Yan Wang, College of Veterinary Medicine, Northwest A&F University, Yangling (712100), China.

Author details

1 College of Veterinary Medicine, Shaanxi Center of StemCells Engineering & Technology, Northwest A&F University, China. 2 Xi'an Animal Hospital, Northwest A&F University, China

References

1. Hua J, Sakamoto I, Fau - K, Nagaoka, Nagaoka I. Inhibitory actions of glucosamine, a therapeutic agent for osteoarthritis, on the functions of neutrophils. J Leukoc Biol. 2002;71(4):632–40.
2. Hamdi A, Hajage E, Fau - D, Van Glabeke X, Van Glabeke E, Fau - Belenfant F, Belenfant X, Fau - Vincent F, Vincent F, Fau - Gonzalez M Gonzalez F Fau - Ciroldi, E. Ciroldi M Fau - Obadia, R. Obadia E, Fau - Chelha J-L. Chelha R Fau - Pallot, V. Pallot Jl Fau - Das and V. Das. Severe post-renal acute kidney injury, post-obstructive diuresis and renal recovery. BJU Int. 110(11 Pt C):E1027-34.(2012).
3. Worwag S, Langston CE. Acute intrinsic renal failure in cats: 32 cases (1997–2004). J Am Vet Med Assoc. 2008;232(5):728–32.
4. Grange C, Skovronova R, Marabese F. and B. Bussolati. Stem Cell-Derived Extracellular Vesicles and Kidney Regeneration. Cells. 2019;8(10):1240.
5. Thongboonkerd V. Roles for Exosome in Various Kidney Diseases and Disorders. Front Pharmacol. 2019;10:1655.
6. Matera M, Bellinghieri G, Fau - G, Costantino D, Costantino G, Fau - Santoro M. Santoro D. Fau - Calvani, V. Calvani M Fau - Savica and V. Savica. History of L-carnitine: implications for renal disease. J Ren Nutr. 2003;13(1):2–14.
7. Liu Y, Yan C, Fau - S, Ji W, Ji C, Fau - Dai W, Dai W, Fau - Hu W. Hu W, Fau - Zhang C, Zhang W, Fau - Mei, Mei C. Metabolomic changes and protective effect of (L)-carnitine in rat kidney ischemia/reperfusion injury. Kidney Blood Press Res. 2012;35(5):373–81.
8. Park J, Lee Sy Fau A - Ooshima K-M, Ooshima A, Fau - Yang JM Yang Km Fau - Kang, Y.-W. Kang Jm Fau - Kim, S.-J. Kim Yw Fau - Kim and Kim SJ, Glucosamine hydrochloride exerts a protective effect against unilateral ureteral obstruction-induced renal fibrosis by attenuating TGF-β signaling. J Mol Med (Berl). 91(11):1273-84.(2013).
9. Visek WJ. Nitrogen-stimulated orotic acid synthesis and nucleotide imbalance. Cancer Res. 52(7 Suppl):2082s-2084s.(1992).
10. Lee GC, Lin CH, Tao YC, Yang JM, Hsu KC, Huang YJ, Huang SH, Kung PJ, Chen WL, Wang CM, Wu YR, Chen CM, Lin JY, Hsieh-Li HM. and G. J. Lee-Chen., The potential of lactulose and melibiose, two novel trehalase-indigestible and autophagy-inducing disaccharides, for polyQ-mediated neurodegenerative disease treatment. Neurotoxicology. 48:120 – 30.(2015).
11. Lin CH, Wei PC, Chen CM, Huang YT, Lin JL, Lo YS, Lin JL, Lin CY, Wu YR, Chang KH. and G. J. Lee-Chen. Lactulose and Melibiose Attenuate MPTP-Induced Parkinson's Disease in Mice by Inhibition of Oxidative Stress, Reduction of Neuroinflammation and Up-Regulation of Autophagy. Front Aging Neurosci. 2020;12:226.

12. He L, Zhang F, Jian Z, Sun J, Chen J, Liapao V, He Q. Stachyose modulates gut microbiota and alleviates dextran sulfate sodium-induced acute colitis in mice. Saudi J Gastroenterol. 2020;26(3):153–9.
13. Liu Y, Fau - Li T, Li A, Fau - T, Alim D, Alim A, Fau - Ren Y, Ren DF - Zhao X, Zhao Y. Fau - Yang and X. A.-O. Yang. Regulatory Effects of Stachyose on Colonic and Hepatic Inflammation, Gut Microbiota Dysbiosis, and Peripheral CD4(+) T Cell Distribution Abnormality in High-Fat Diet-Fed Mice. J Agric Food Chem. 2019;67(42):11665–74.

Supplemental Data

Tables S1 and S2 are not available with this version

Figures

Figure 1

The male cat model of artificial urethral blockage mimics the clinical symptoms of PR-AKI A. Schematic diagram of a male cat model of artificial urethral blockage. B. Dynamic changes of creatinine (CRE) levels at different time points of artificial urethral blockage in male cats. C. B-ultrasound imaging of kidney in male cats with artificial urethral obstruction for 48 hours. D Pathological section HE staining of kidney in male cats with artificial urethral obstruction for 48 hours. E The proportion of lesion area in pathological sections.

Figure 2

Efficacy comparison of control and exosomes in the treatment of PR-AKI cats. A. ADMSCs morphology and its differentiation into adipose and cartilage identified by oil red staining and alizarin red staining, respectively. B. Transmission electron microscopy identification of ADMSCs-derived exosomes. C. Western blotting identification of ADMSCs-derived exosomes marker proteins (TSG101, CD63). D. Schematic diagram of different treatment procedures for PR-AKI cats. E. Dynamic fold changes of leukocyte number in PR-AKI cats treated by different methods. F-H. Dynamic fold changes of creatinine (F), urea nitrogen (G), plasma phosphorus (H) of PR-AKI cats treated with different methods. I. Fold changes of body temperature in PR-AKI cats treated by different methods.

Figure 3

Plasma metabonomics of PR-AKI cats treated with ADMSCs-derived exosomes. A-B. Principal component analysis of positive ion features (A) and negative ion features(B). C. Volcano diagram of differential metabolic compounds (annotated from positive ion features) between PR-AKI cats and normal group. D. Volcano diagram of differential metabolic compounds (annotated from positive ion features) between ADMSCs-derived exosomes treatment group and normal group. E. Volcano diagram of differential metabolic compounds (annotated from negative ion features) between PR-AKI cats and normal group. F. Volcano diagram of differential metabolic compounds (annotated from negative ion features) between ADMSCs-derived exosomes treatment group and normal group.

Figure 4

Potential targets of ADMSCs-derived exosomes in the treatment of PR-AKI. A. KEGG pathway analysis of significantly up-regulated compounds (annotated from positive ion features) in PR-AKI group compared with normal group. The compounds enriched in the pathways with significant difference ($p<0.05$) are listed on the right panel. Similar presentation of enriched compounds in the pathways with significant difference are applied in B, C, D. B. KEGG pathway analysis of significantly down-regulated compounds (annotated from positive ion features) in exosome treatment group compared with PR-AKI group. C. KEGG pathway analysis of significantly up-regulated compounds (annotated from negative ion features) in PR-AKI group compared with normal group. D. KEGG pathway analysis of significantly down-regulated compounds (annotated from negative ion features) in exosome treatment group compared with PR-AKI group. E. Heatmap showing the expression abundance of six compounds as potential targets for ADMSCs-derived exosomes treatment of PR-AKI.

Figure 5

Correlation and linear regression analysis of six compounds with clinical indicators of PR-AKI. A. Heatmap showing the correlation coefficients between six compounds and clinical indicators (creatinine, urea nitrogen, and plasma phosphorus) of PR-AKI. The coefficient of determination and linear regression equation are labeled for each analysis. Similar labels are also applied in B, C, D. B. Linear regression analysis of six compounds and creatinine. C. Linear regression analysis of six compounds and urea nitrogen. D. Linear regression analysis of six compounds and plasma phosphorus.

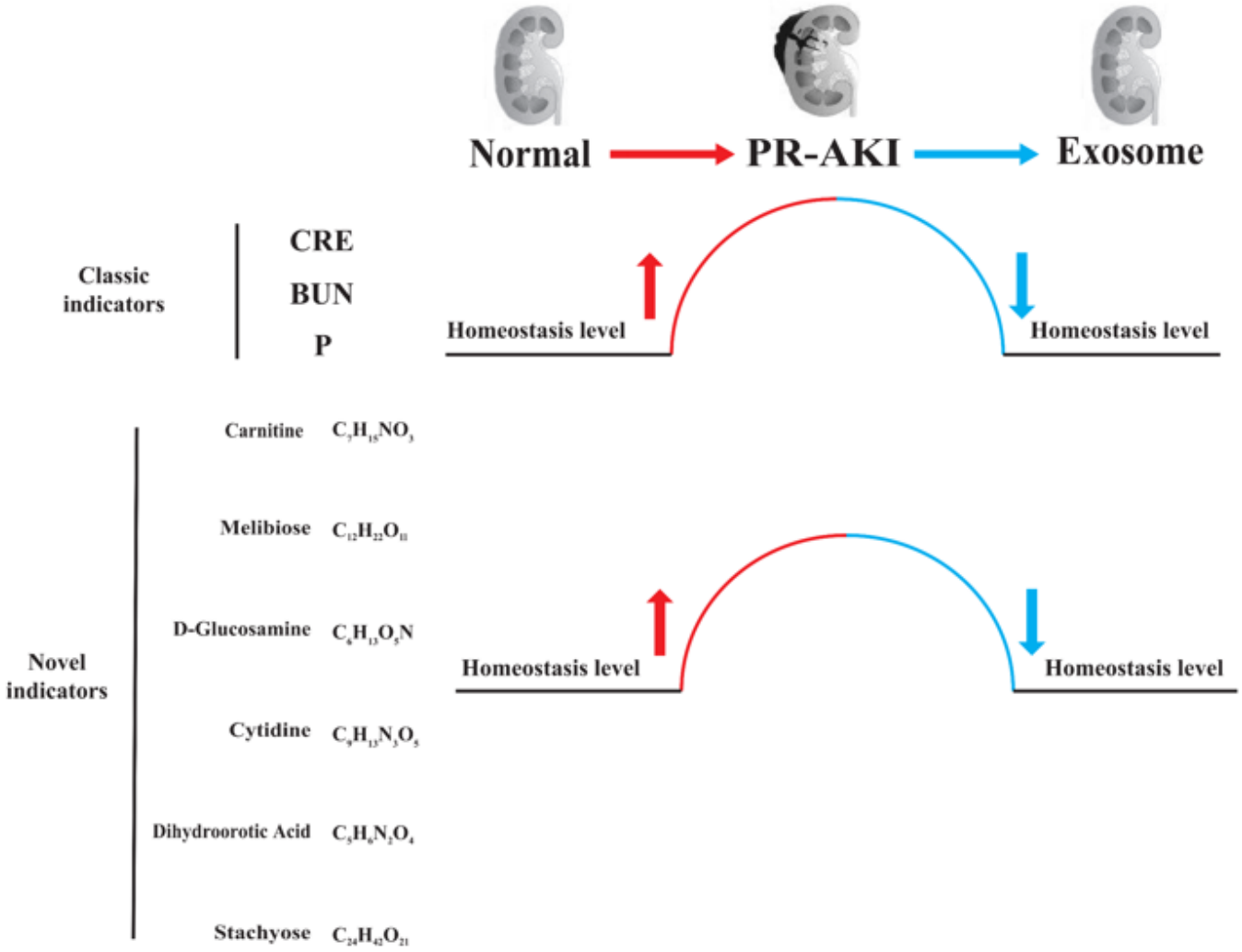

Figure 6

The changes of three classical markers and six novel markers in the pathogenesis and prognosis of PR-AKI.

Supplementary Files

This is a list of supplementary files associated with this preprint. Click to download.

- SupplFigure1.docx